

A hybrid optimization-agent-based model of REDD+ payments to households on an old deforestation frontier in the Brazilian Amazon

Thales A.P. West ^{a,*}, Kelly A. Grogan ^b, Marilyn E. Swisher ^c, Jill L. Caviglia-Harris ^d, Erin Sills ^e, Daniel Harris ^f, Dar Roberts ^g, Francis E. Putz ^h

^a School of Natural Resources and Environment, University of Florida, Gainesville, FL 32641, USA

^b Food and Resource Economics Department, University of Florida, Gainesville, FL 32641, USA

^c Family, Youth and Community Sciences Department, University of Florida, Gainesville, FL 32641, USA

^d Economics and Finance Department, Salisbury University, Salisbury, MD 21801, USA

^e Department of Forestry and Environmental Resources, North Carolina State University, Raleigh, NC 27695, USA

^f Department of Geography and Geosciences, Salisbury University, Salisbury, MD 21801, USA

^g Department of Geography, University of California, Santa Barbara, CA 93106, USA

^h Department of Biology, University of Florida, Gainesville, FL 32641, USA



ARTICLE INFO

Article history:

Received 9 March 2017

Received in revised form

25 August 2017

Accepted 8 November 2017

Available online 23 November 2017

Keywords:

REDD+

Payments for environmental services

Land-use/cover change

Agent-based modeling

Farm household

Optimal control

ABSTRACT

REDD+ was initially conceived of as a multi-level carbon-based payment for environmental services (PES). It is still often assumed to be a cost-effective climate change mitigation strategy, but this assumption is mostly based on theoretical studies and static opportunity cost calculations. We used spatial and socioeconomic datasets from an Amazonian deforestation frontier in Brazil to construct a simulation model of REDD+ payments to households that can be used to assess REDD+ interventions. Our *SimREDD+* model consists of dynamic optimization and land-use/cover change allocation sub-models built into an agent-based model platform. The model assumes that households maximize profit under perfect market conditions and calculates the optimal household land-use/cover configuration at equilibrium under a given REDD+ PES scenario. These scenarios include PES based on (1) forest area and (2) carbon stocks. Insights gained from simulations under different conditions can assist in the design of more effective, efficient, and equitable REDD+ programs.

© 2017 Elsevier Ltd. All rights reserved.

Software and/or data availability

The model described, *SimREDD+*, was built in NetLogo v.5.3.1 software for agent-based modeling (Wilensky, 1999). The first and current version of the model was finalized in October 2016. NetLogo, and therefore *SimREDD+*, should work on any platform on which Java 5 or later is installed. Computers with <8 GB of RAM might run out of memory due to the substantial number of virtual agents simulated in the model. *SimREDD+* script is freely available from the corresponding author after signature of a *Data Use Agreement* between the requester, the corresponding author, and the Principal Investigators responsible for acquisition of the sensitive household-level socioeconomic data.

1. Introduction

Spatially explicit biophysical and anthropogenic factors correlated with tropical deforestation are well discussed in the literature (e.g., Geist and Lambin, 2002; Müller et al., 2012; Pfaff, 1999) and are often key components of land-use/cover change (LUCC) simulation models (Eastman, 2015; Soares-Filho et al., 2002). Examples of these factors are land slopes and distances from roads, markets, and protected areas. The observation that the relationships among such factors shed little light on the decision-making processes that undergird LUCC (Deadman et al., 2004; Le et al., 2008; Parker et al., 2003) motivates attempts to elucidate the causal effects of policy interventions on deforestation (e.g., Blackman, 2013; Börner et al., 2016). One way to remedy this deficiency is through use of agent-based models (ABM), which offer a powerful way to explore coupled human-natural complex systems (Wilensky and Rand, 2015). ABMs can be used, for example, to inform the design of policies or programs to curb deforestation while minimizing

* Corresponding author.

E-mail address: thaleswest@gmail.com (T.A.P. West).

negative impacts on local stakeholders (Iwamura et al., 2016; Purnomo et al., 2013; Snistveit et al., 2016). In this paper, we describe a hybrid optimization-ABM that simulates the effects of payments for environmental services (PES) to settlers on an old Amazonian deforestation frontier on LUCC and community welfare. Payments were structured in accordance with REDD+ (Reducing Emissions from Deforestation and Forest Degradation, with recognition of the roles of conservation, sustainable forest management, and enhancement of carbon stocks; UN-REDD, 2008, 2011) practices. The model presented here was designed to shed light on issues related to the long-run effectiveness, efficiency, and equity of REDD+ interventions.

An ABM is a complexity-theory based computerized simulation (Snooks, 2008) of a number of decision-makers (agents) who interact through prescribed rules in a dynamic environment (An, 2012; Liu et al., 2007). The independence of agents represented in an ABM and their interactions allow researchers to capture characteristics over time of complex systems like heterogeneity, nonlinearity, feedbacks, and emergent properties (An, 2012; An et al., 2005; Liu et al., 2007). ABMs have the potential to assess impacts of policy scenarios on coupled human-natural systems as they attempt to mimic the behavior of institutions and stakeholders in a virtual representation of reality (e.g., Andersen et al., 2014; Iwamura et al., 2014; Purnomo et al., 2013). Thus, development and application of ABMs represent a reasonable early step in policy-making (Farmer and Foley, 2009), which is substantially less costly than field-based randomized-control trials and can provide guidance sooner than quasi-experimental evaluations of pilot initiatives (Sills et al., 2017).

LUCC models based on ABM frameworks are often coupled with biophysical information about the landscape that can be used for spatially-explicit model validation (Deadman et al., 2004; Ngo and See, 2012; Pontius et al., 2011). The spatial component of LUCC-ABM allows for better virtual representation of real landscapes and consideration of both natural and socioeconomic contexts (An et al., 2005; Deadman et al., 2004; Mena et al., 2011). Arguably, the most important component of a LUCC-ABM is the decision-making processes of its virtual agents (e.g., farm households). In general, those processes are based on decision-trees (e.g., Deadman et al., 2004; Salvini et al., 2016) or the maximization of utility functions (e.g., Andersen et al., 2014; Monticino et al., 2007). Maximization problems often include labor, income, and physical constraints (e.g., Evans et al., 2001) and are grounded in farm household economics and agricultural production theories (Angelsen, 1999; Darwin et al., 1996).

REDD+ was initially conceived as a system of PES for carbon retention or sequestration (UN-REDD, 2011). It has garnered substantial international attention as a potentially cost-effective approach to climate change mitigation (Kindermann et al., 2008). Negotiations at the 21st Conference of Parties of the United Nations Framework Convention on Climate Change acknowledged REDD+ as a strategy to be incorporated into future international climate regulations (UNFCCC, 2015). Yet, it is widely accepted that REDD+ will only be effective if payments offset stakeholders' opportunity costs, which can vary substantially (Abram et al., 2016; Borrego and Skutsch, 2014; Torres et al., 2013). A recent meta-analysis by Phan et al. (2014) reported opportunity costs for REDD+ range from US\$0.05 to \$92 Mg CO₂⁻¹. The average cost in Latin America was approximately \$5.4 Mg CO₂⁻¹, within the <\$0.2 to \$13 Mg CO₂⁻¹ range reported by Börner and Wunder (2008) for the Brazilian Amazon. Ickowitz et al. (2017) reported substantially higher opportunity costs to smallholders over a 30-year time horizon with a 9% discount rate, ranging from \$11 to \$77 Mg CO₂⁻¹ across five sites in the Brazilian Amazon. In contrast, Nepstad et al. (2007) use a much lower opportunity estimate of \$1.5 Mg CO₂⁻¹

across the entire region.

Multiple reasons explain why opportunity costs range so widely across the tropics, but the primary one stems from variation in possible land uses. Not all tropical forests are located in plantations due to logistical (e.g., inaccessible regions) or environmental reasons (e.g., soil quality, precipitation regimes, and presence of phytopathogens). In addition, the lack of high-quality spatial and economic data to estimate opportunity costs often forces researchers to extrapolate them from one region to others with very different conditions, land use options, and opportunity costs (e.g., Börner et al., 2014; Nepstad et al., 2007), which could result in inaccurate estimates. Furthermore, when opportunity cost estimates are static, i.e., they are not allowed to change with changes in economic conditions over time (Pana and Gheysens, 2016; Takasaki, 2012), interpretation of results must be made with extra caution. Given that market conditions can change substantially over time, more dynamic analyses are warranted. ABMs can shed light on the extent to which different REDD+ payments are likely to change business-as-usual behavior through time by simulating LUCC decision-making by farm households, which avoids the potential pitfalls of static opportunity cost analyses (Andersen et al., 2014; Purnomo et al., 2013; Salvini et al., 2016).

Here we describe a hybrid optimization-ABM (e.g., Andersen et al., 2014) we developed to evaluate the potential impacts of REDD+ payments on settlers on an Amazonian deforestation frontier. Impacts are evaluated in terms of land-use/cover change, CO₂ emissions, total program expenditures on PES given program enrollment rates, and community welfare. Even though our model was constructed on an ABM platform, we consider it a hybrid model because agents' LUCC decisions are strictly based on the solution of the dynamic optimization problem in which each household seeks to maximize farm profits.

2. Methods

2.1. Study region

The study region covers approximately 6000 km² in Rondônia State, Brazil, including the municipality of Ouro Preto do Oeste and its five contiguous neighbors, Vale do Paraíso, Nova União, Teixeirópolis, Urupá, and Mirante da Serra, all of which are near the major federal highway, BR-364 (Fig. 1). The area lies within the "arc of deforestation" in the Brazilian Amazon (Caviglia-Harris, 2005), a well-documented heavily deforested old frontier where settlers began arriving in the 1960s in response mostly to government-sponsored programs. These include the "National Integration Program," the "Northwest Region Integrated Development Program," and "Operation Amazonia" (Caviglia-Harris, 2004; Sills and Caviglia-Harris, 2008). In the study region, the federal land reform agency, INCRA, allocated nearly 9000 lots laid out in a regular pattern along roads to settlers arriving from other regions. Deforestation in the study region has therefore followed a road-related "fishbone" pattern, and has been the subject of numerous LUCC studies since the early 1990s (e.g., Dale et al., 1994).

2.2. Datasets

2.2.1. Socioeconomic data

Socioeconomic household survey data from a systematic random sample stratified by municipality collected from 697 households in 2009 were used to parameterize the model (Caviglia-Harris et al., 2014). The majority of households in the region, virtually all of which immigrated from outside the Amazon, are small-scale producers (98%) with an average property size of 65 ha (range: 2–240 ha), while the average for medium and large lots

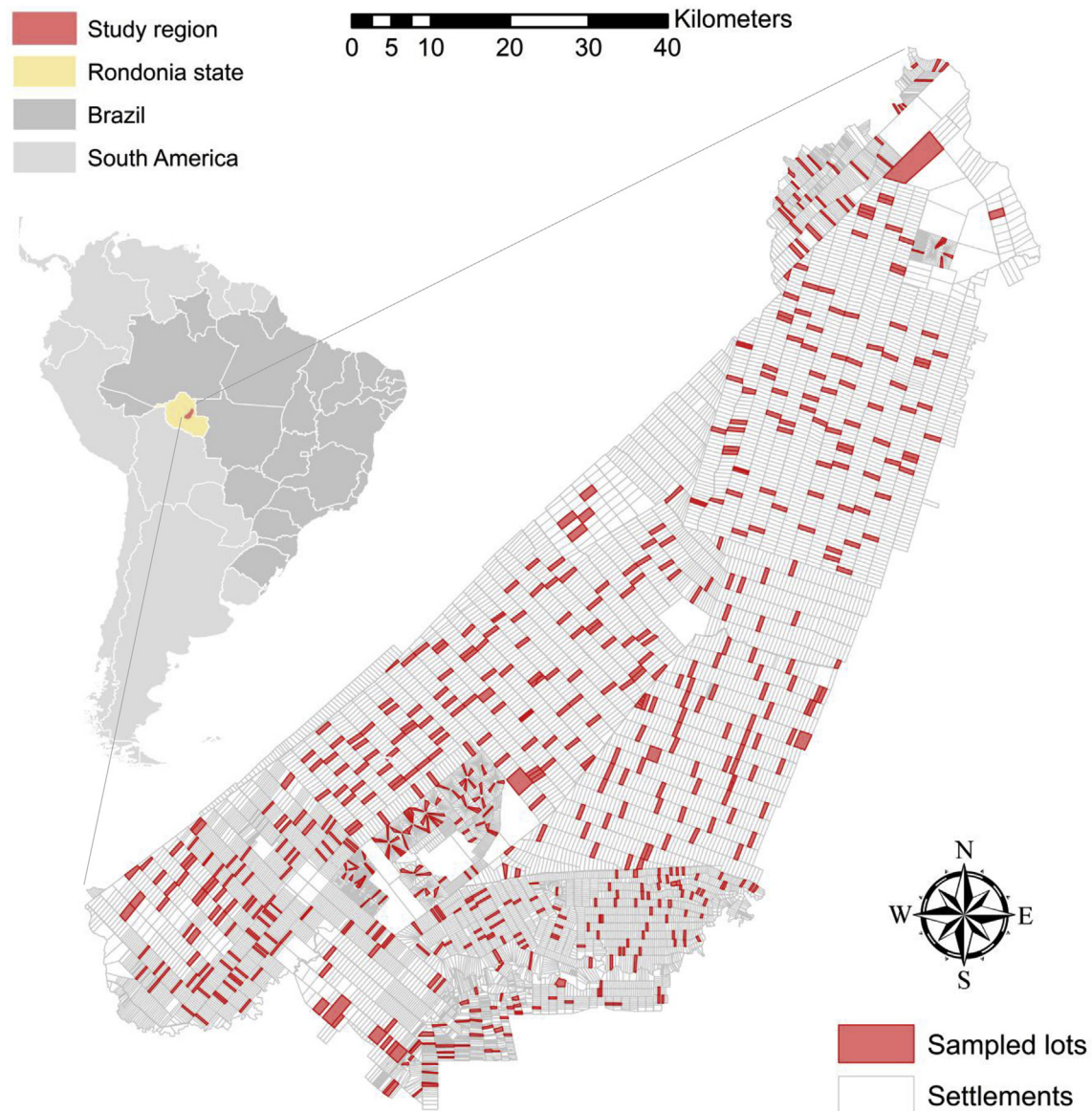


Fig. 1. Study region.

(top 2%) is 745 ha (range: 240–3000 ha). Households initially focused on annual and perennial crops, but revenues from these crops declined by almost 70% between 1996 and 2009 and dairy and beef cattle production largely replaced that income. Milk production increased from an average of approximately 17,000 L per year in 1996 to approximately 30,000 L in 2009. Overall, annual income per household increased from \$4000 to more than \$9000 (inflation-adjusted) for the same period and the average number of cattle owned per household increased from approximately 70 to 140 head. The settlements experienced high rates of deforestation between 1996 and 2009, with mature forest cover decreasing by more than 50%. Overall, only about 10% of forest cover remained in the study region in 2009 (Caviglia-Harris and Harris, 2011; Caviglia-Harris et al., 2015).

2.2.2. Remote sensing and GIS data

The hybrid model incorporates a spatially explicit LUCC sub-model based on five spatial layers. (1) The first is a map displaying the location of 8900 settlement properties (Caviglia-Harris et al.,

2015, Fig. 1). (2) The second is a Landsat 5 satellite-based LUCC classification map generated in 1996, the year the first survey was completed, showing mature forest, secondary forest (i.e., forest that regenerated naturally after abandonment of agricultural land), and agricultural use classes (Fig. S1; Roberts et al., 2002; Toomey et al., 2013). (3) The third map, created using the artificial neural network-based algorithm, shows the ranked suitability (i.e., “risk”) for deforestation of mature forest patches. The deforestation suitability map was constructed with the *Multi-Layer Perceptron* (MLP), an artificial neural network-based algorithm available in TerrSet v.18.11 software (Eastman, 2015). It indicates the forest patches within the study region that are more likely to be cleared in the future (Fig. S2). The map was based on the mapped land-use/cover changes and persistence between 1986 and 1996 and 11 biophysical maps of the study region. The maps included in the MLP were: administrative areas at the municipality level; macro-political regions; soil quality; elevation; timber market zones; distances from previously deforested areas; distance from major roads; distance from major rivers; distance from protected areas; distance from

logging areas; and, distance from major markets (Table S1 and Fig. S3). The calibration accuracy of the MLP was 71% (Table S2). (4) The fourth is a map of ranked suitability of secondary forest clearing based on Euclidian distances to agricultural land in 1996. (5) The final map provides the ranked suitability of agricultural abandonment based on Euclidian distances to forest patches in 1996. Additionally, the tropical carbon-density map developed by Baccini et al. (2012) was used to estimate per-hectare averages of net carbon emissions from LUCC (Figs. S4 and S5).

2.3. Model description

The LUCC model, named *SimREDD+*, is described in accordance to the Overview, Design concepts, and Details (ODD) protocol, a standard guideline for the description of ABMs (Grimm et al., 2010). *SimREDD+* was built in NetLogo v.5.3.1 (Wilensky, 1999). General data analyses were conducted with R v.3.3.0 statistical software (R Core Team, 2016). Algebraic transformations were performed in Mathematica v.9.0 (Wolfram Research, Inc., 2012). Spatial analyses were conducted with R, TerrSet v.18.11 (Eastman, 2015), and ArcGIS v.10.3.1 (ESRI, 2015) software.

2.3.1. Purpose

The model aims to simulate the effects of direct REDD + payments conditional on forest cover, including both retention of mature forest and regeneration of secondary forest. The objective of the model is to assist in the design of more effective, efficient, and equitable REDD + programs and policies in the long run. The first step in the model is to create a baseline LUCC scenario at equilibrium without REDD + payments. The second step introduces REDD + payments as an additional source of annual income for households. Payments are proportional to the sum of the area in mature forest and the area set aside for secondary forest regrowth on each property. Given a PES scenario, households choose a new optimal land-use/cover configuration. Based on estimates of carbon stocks associated with each land-use/cover class, the model quantifies net carbon emissions (Mg CO₂) from the LUCC activities.

Two types of PES for forest conservation are often discussed in the literature: (1) payments based on forest carbon stocks; and, (2) payments based on forest area. The first scheme is associated to carbon market-based initiatives (e.g., Hamrick and Goldstein, 2016), while the second approach is often taken by government conservation programs (e.g., Arriagada et al., 2012; de Koning et al., 2011). *SimREDD +* can simulate these two PES schemes. REDD + payments under the *carbon market option* are applied in accordance with decentralized/private PES for avoided deforestation and voluntary carbon market rules that are expected to be followed by national REDD + programs (Verified Carbon Standard, 2017a). REDD + payments based on area (\$ ha⁻¹) are referred to as the *policy option* in *SimREDD+* and are assumed to be annual, constant, and based on the current area of mature forest cover plus agricultural areas set aside for secondary forest regrowth on each property. In practical terms, the implementation of PES policy option is easier when compared to the carbon market option described above as it does not require estimation of forest carbon stocks. Under the carbon market option, REDD + payments are based on the differences in carbon emissions under the baseline and project scenarios (\$ Mg CO₂⁻¹). This option also assumes that REDD + payments for a given ton of CO₂ either removed or not emitted to the atmosphere (i.e., additional CO₂) are made only once during a hypothetical carbon project lifetime, in accordance with carbon market standards (Verified Carbon Standard, 2017b). The project lifetime considered in our simulations is 20 years. Constant renewal of the hypothetical carbon project is assumed after

expiration because the model is projected into infinity. As result, a given ton of additional CO₂ is rewarded multiple times, but only once every 20 years. Therefore, a direct implication of changing the hypothetical carbon project lifetime is that, if length <20 years, a given ton of additional CO₂ is rewarded more frequently in the long term and hence REDD + revenues for the household increases. The opposite effect is observed if the length of the project is > 20 years. It is our understanding that these two schemes encompass the majority of currently implemented PES interventions focused on forest conservation and restoration.

In accordance with the framework of the United Nations' collaborative program on REDD+ (UN-REDD, 2015), the model considers but makes no distinctions between payments made for avoided deforestation and promotion of natural regeneration. This simplification seems justified because secondary forests present at the beginning of model simulations (in 1996) and newly formed forest patches created through the abandonment of agricultural land are both assumed to reach the status of mature forests when projected into infinity, when no LUCC occurs at model equilibrium (see Section 2.3.6 and the Supplementary Material for details). The model reports the total annual amount of money spent by the simulated REDD + scheme on PES at equilibrium. The model assumes that enrollment is voluntary and unconstrained and that the amount of land households allocate to REDD+ (if any) depends on the extent to which the offered PES offset the households' opportunity costs. The model does not incorporate the total cost of the REDD + interventions as it does not capture transaction or administrative costs (Luttrell et al., 2017; Thompson et al., 2013).

2.3.2. Entities, state variables, and scales

There are two types of entities in the model, households (or farmer-agents) and land-use/cover patches (28.5 m resolution). The approximately 6000 km² of settlements were divided into ten sub-regions to cope with the computational limitations of NetLogo (Railsback et al., 2006; Fig. S6; Table S3). Agricultural patches represent different and unspecified mixes of annual and perennial crops and pasture. Three variables describe each patch (grid cell) in the model: (1) a land-use/cover category (mature forest, secondary forest, or agriculture); (2) a patch-owner identification number; and, (3) a value related to its suitability of change to a different land-use/cover class (either the "risk" of deforestation for forest patches or of abandonment for agricultural patches).

Aboveground carbon stocks were estimated in Mg CO₂ ha⁻¹, the standard unit of carbon emission offsets (Rifai et al., 2015; UNFCCC, 2013a), based on the weight ratio between CO₂ and C (44/12), a biomass carbon fraction of 0.47, and below-to aboveground biomass ratios of 0.24 and 0.20 for mature and secondary forest, respectively (IPCC, 2006; Mokany et al., 2006). The averages of aboveground carbon stocks associated with the mature and secondary forest land-cover classes were estimated at 537 and 418 Mg CO₂ ha⁻¹, respectively (Baccini et al., 2012; Fig. S4). For agricultural patches, a total carbon stock at equilibrium of 104 Mg CO₂ ha⁻¹ was adopted (Fearnside, 1996). Farmer-agents are assigned a patch-owner identification number that indicates which patches they own and the size of their farms. Farms are not allowed to change sizes over the course of the simulation (i.e., household members do not split or acquire lots).

2.3.3. Process overview and scheduling

The model represents two processes related to LUCC in the settlements. The first is quantification of the optimal agricultural area for each farm. The second is the spatial allocation of deforestation of forest patches and abandonment of agricultural patches. Shifts in the optimal agricultural area result from changes in the parameter values displayed on the model interface: market price of

agricultural outputs; REDD + payments for avoided deforestation and promotion of natural regeneration; and, wage rates. Simulations end when the LUCC equilibrium state is reached, as defined by the individual farmer-agents' optimal agricultural area under each payment scenario.

2.3.4. Design concepts

Basic principles: The model is based on the theory of farm households operating in complete markets (Darwin et al., 1996) in which households are assumed to behave as if they maximize profits (Angelsen, 1999; Takasaki, 2013). These farm households are the farmer-agents in the model. A Cobb-Douglas production function is embedded into the farmer-agent's profit function. The literature on farm household production is generally focused on one crop to avoid problems often encountered in multicrop production models (Barnum and Squire, 1979). In light of this limitation and to make the LUCC model as generalizable as possible, the rice-equivalent (Andersen et al., 2014) was adopted as a single standard agricultural output. Annual and perennial crops, as well as animal production, and their respective prices were converted into their rice-equivalent based on energy content and annual productivity (Tables S4 and S5; Fig. S7).

Emergence: LUCC patterns emerge based on the optimal agricultural area calculation and the areas more suitable for land-use/cover change and persistence due to the fact that transitions of one patch affect the suitability for transitions of neighboring patches.

Adaptation/learning: Agents do not present adaptive traits (i.e., they do not change behavior over time in response to learning).

Objective: The farmer-agent's objective is to maximize a profit function through a dynamic optimization framework. A Cobb-Douglas production function (e.g., Barnum and Squire, 1979) determines the volume of rice-equivalents produced as a function of the household's agricultural area and labor. Predicted production combined with agricultural output prices determine the households' revenue. The model assumes that a given agricultural patch maintains the same productivity into infinity, which is an average of the production potential of the agricultural land obtained from the panel data through an ordinary-least squares regression. Maintenance costs of agricultural patches, deforestation costs, and labor costs are subtracted from household revenue. In cases that incorporate REDD + payments, the latter are added to household profit.

Prediction/Sensing: Households are treated as homogenous agents. They are aware of the patches within their farms' boundaries, the current land-use/cover class of those patches, and the suitability of mature and secondary forest patches for deforestation or of agricultural patches for abandonment. Through the dynamic optimization exercise, the farmer-agents become aware of the optimal size of agricultural area and change their land-use/cover patches to reach that level.

Interaction/collectives: Land-use/cover patches belong to a farm and a farmer-agent. Farmer-agents interact exclusively with their own land-use/cover patches with no interactions among households. Nonetheless, neighboring patches influence the suitability of LUCC of areas that belong to different farmer-agents.

Stochasticity: No stochastic processes are incorporated in the model. The initialization conditions are based on a LUCC classification map of 1996, while the dynamic optimization process is based on an internal analytical solution. Both procedures are deterministic.

Observations: Changes in areas of forest and agricultural land at the sub-region level in the simulation are monitored and compared to the areas in LUCC classification maps derived from Landsat satellite imagery. Annual household profits at the equilibrium state of

the model run are also monitored and compared to the 2009 panel data survey.

2.3.5. Initialization

The model is run for one of its ten sub-regions at a time, with one farmer-agent created for each farm. Land-use/cover patches are created following a Landsat 5-based LUCC classification map from 1996 (Roberts et al., 2002; Toomey et al., 2013). Deforestation and abandonment suitability maps are loaded into NetLogo and their values are assigned to forest and agricultural patches, respectively. Similarly, land-use/cover patches are assigned to their respective farmer-agent owners. The farmer-agents count the patches in each land-use/cover class within their farms and store those values for use during the model run. NetLogo then displays the 1996 land use/cover map on which it overlays property boundary polygons (Fig. 2). Finally, initial sizes (ha) of mature forests, secondary forests, and agricultural lands at the landscape level are reported and community welfare is calculated as the sum of all households' annual farm profit.

2.3.6. Submodels

Profit maximization submodel: The household decision-making process is assumed to follow a dynamic maximization framework. Such a framework is required because any additional deforestation expands the household agricultural area. Households maximize a profit function under perfect labor market conditions (Angelsen, 1999; Takasaki, 2013):

$$\Pi = p_A f(A_t, L_t) + p_{E_i}(F - A_t) - w(L_t + \gamma D_t) - C_A A_t - C_D D_t \quad (1)$$

where p_A is the price of the agricultural production output; $f(A_t, L_t)$ is the production function that predicts output produced as a function of agricultural area (A_t) and agricultural labor (L_t) at time t ; w is the wage rate associated with agricultural labor and the deforestation and site preparation labor (γ) per unit of deforested area (D_t); C_A and C_D are non-labor costs associated with maintaining agricultural areas (A_t); and deforestation and site preparation costs required per hectare of deforested area (D_t), respectively. The profit function also incorporates the financial benefit from an environmental service payment represented by $p_{E_i}(F - A_t)$, where p_{E_i} is the REDD + payment (\$ unit $^{-1}$) for payment type i (discussed further below) based on the total farm area (F) not converted for agricultural land use (A_t), under the assumption that all farms were once forested. To allow an analytical solution, a Cobb-Douglas production function was chosen for its closed-form solution property (e.g., Angelsen, 1999; Bronfenbrenner and Douglas, 1939):

$$f(A_t, L_t) = \alpha A_t^\beta L_t^\varphi \quad (2)$$

where β and φ are the land area and labor output elasticities, respectively, and α is the total factor of productivity. These three parameters were estimated from the socio-economic panel data based on the agricultural area and family size of the household, number of family members with off-farm jobs, and number of people hired to work on the farm throughout a year. Given that production functions are likely to vary with property size, production function parameters were estimated based on data from small farms, with 28 large lots excluded from the simulations. Among the excluded farms are shared *Legal Reserves* that belong to the settlements (areas that must remain forested to comply with Brazilian environmental regulations).

The unit of p_{E_i} varies with the REDD + payments scheme (i) chosen. With the REDD + policy option, payments, p_{E_p} , are based on the remaining mature forest area and the area allocated for secondary forest regrowth in the farm (\$ ha $^{-1}$). With the carbon

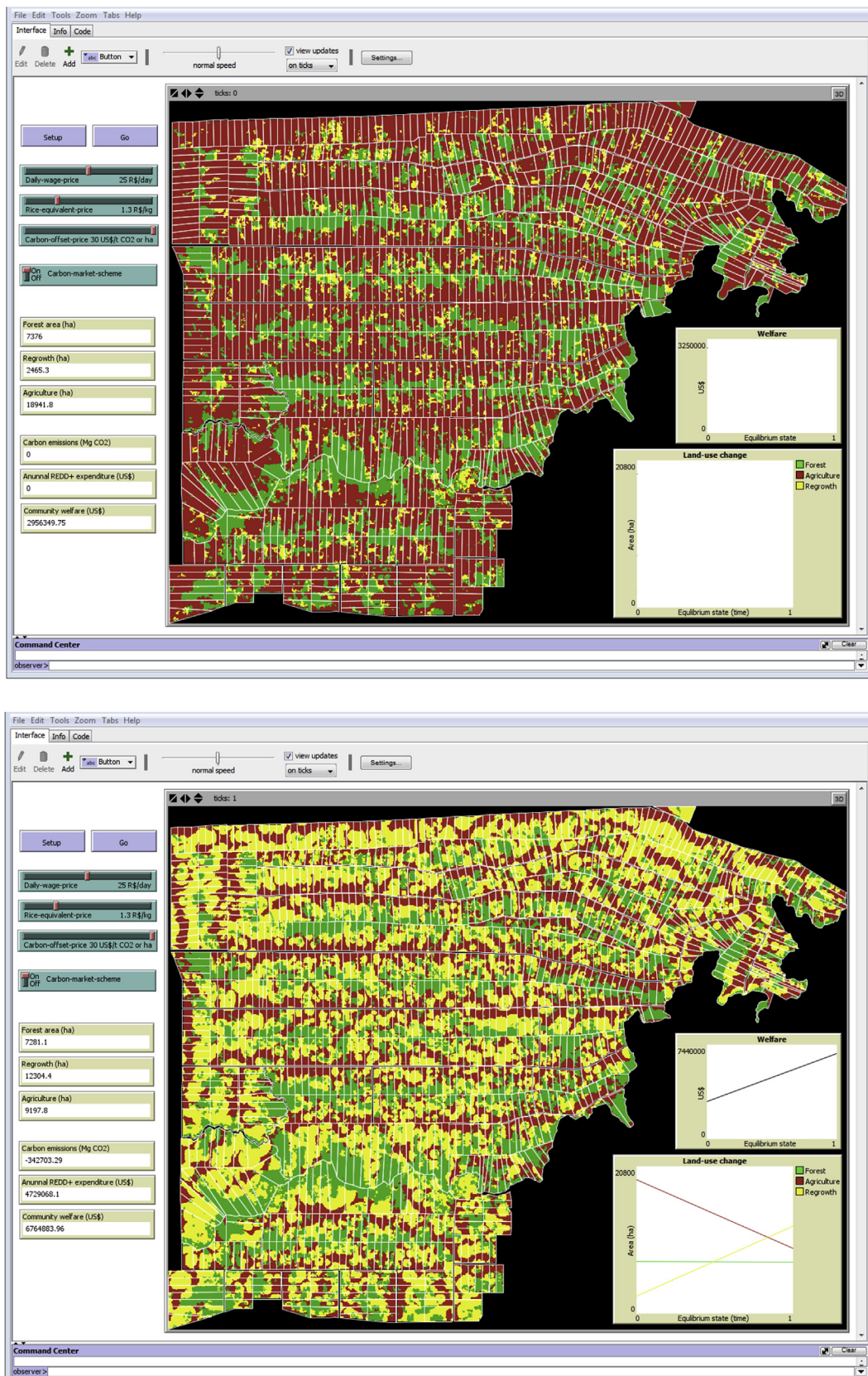


Fig. 2. Initialization interface (upper panel) and simulation output (lower panel) for the Urupá 1 sub-region.

market option, payments, p_{E_μ} , are based on the net carbon emissions from avoided conversion of forest to agricultural land and net carbon sequestration from regeneration of abandoned agricultural patches (Mg CO_2^{-1}), captured by an additional term δ (Rifai et al., 2015). Because payments for a given Mg CO₂ can only occur once over a carbon project lifetime, the average annual REDD + payment under the carbon market scheme becomes:

$$p_{E_\mu} = \frac{p_{E_\mu} \delta}{T} \quad (3)$$

where T represents a hypothetical REDD + project lifetime implemented in accordance with voluntary carbon market standards (Verified Carbon Standard, 2017b). REDD + payments are annualized by T , which is the time assumed for agricultural patches set aside for forest regrowth to achieve the carbon stock status of mature forest. T years is also the *ex ante* time assumed for all forest patches within a given farm to be cleared in the absence of REDD + payments (see Figs. S8 and S9 for details). Given that $A_t = A_{t-1} + D_t$, the deforestation process is captured as:

$$\frac{\partial A_t}{\partial t} = \dot{A}_t = D_t \quad (4)$$

Additionally, the amount of deforestation cannot exceed the amount of remaining forest, yielding an additional constraint:

$$F - A_t - D_t \geq 0 \quad (5)$$

The optimal solution can be solved with the construction of the following Hamiltonian equation (Michel, 1982):

$$H = p_A \alpha A_t^\beta L_t^\phi + p_{E_i} (F_t - A_t) - w(L_t + \gamma D_t) - C_A A_t - C_D D_t + \lambda_t D_t + \psi(F - A_t - D_t) \quad (6)$$

where λ_t is the co-state variable associated with the expansion of agricultural land and ψ is the shadow value for the maximum deforestation constraint (i.e., households cannot clear more land than they possess). The first-order conditions of the Hamiltonian equation then become:

$$\frac{\partial H}{\partial L_t} = p_A \phi \alpha A_t^\beta L_t^{\phi-1} - w = 0 \quad (7)$$

$$\frac{\partial H}{\partial D_t} = -w\gamma - C_D + \lambda_t - \psi = 0 \quad (8)$$

$$\frac{\partial H}{\partial A_t} = -p_A \beta \alpha A_t^{\beta-1} L_t^\phi + p_E \delta + C_A + \psi = \dot{\lambda}_t - r\lambda_t \quad (9)$$

$$\frac{\partial H}{\partial \lambda_t} = D_t = \dot{A}_t \quad (10)$$

$$\frac{\partial H}{\partial \psi} = \begin{cases} F - A_t - D_t = 0, & \psi > 0 \\ F - A_t - D_t > 0, & \psi = 0 \end{cases} \quad (11)$$

The optimal agricultural land at equilibrium (A^*) is given recursively by solving the optimal control problem (Appendix A):

$$A_t^* = \left(\frac{w \beta^{1-\frac{1}{\phi}} \alpha^{-\frac{1}{\phi}} p_A^{-\frac{1}{\phi}} (rC_D + p_E \delta + C_A + r\psi\gamma + r\psi + \psi)^{\frac{1}{\phi}-1}}{\phi} \right)^{\frac{\phi}{\beta+\phi-1}} \quad (12)$$

In all of the above equations, $\psi = 0$ when there is forest left (i.e.,

the land restriction is not binding). Finally, the deforestation path (D_t) is defined by:

$$D_t = \begin{cases} 0, & w\gamma + C_D + \psi > \lambda_t \\ D^*, & w\gamma + C_D + \psi = \lambda_t \\ \bar{D}, & w\gamma + C_D + \psi < \lambda_t \end{cases} \quad (13)$$

If $A_t < A^*$, the household deforests at the maximum possible rate, \bar{D} . If $A_t > A^*$, the household abandons agricultural land, leading to natural regeneration of forest until the optimal amount of agricultural land is reached. Once the optimal area in agricultural use is reached, deforestation (D_t) equals zero and the amount of agricultural land remains at A^* . While this model assumes parameters to remain constant over time, the model can easily calculate a new equilibrium land area and the associated implied deforestation or forest regeneration if conditions were to change after initial equilibrium is reached.

Optimal agricultural labor at equilibrium (L^*) is then calculated recursively from the profit function (Equations (1) and (2)) given the optimal agricultural area (A^*) as:

$$\Pi = p_A \alpha (A^*)^\beta L_t^\phi + p_{E_i} (F - A^*) - w(L_t + \gamma D_t) - C_A A^* - C_D D_t \quad (14)$$

$$\frac{\partial \Pi}{\partial L_t} = p_A \frac{\partial \alpha (A^*)^\beta L_t^\phi}{\partial L_t} - w = p_A \phi \alpha (A^*)^\beta L_t^{\phi-1} - w = 0 \quad (15)$$

$$L^* = \left(\frac{w}{p_A \phi \alpha (A^*)^\beta} \right)^{\frac{1}{\phi-1}} \quad (16)$$

Finally, the optimization submodel calculates community welfare, based on the sum of all N individual annual household (i) profits for each simulation scenario (j) at the LUCC equilibrium state (Π_E):

$$\Pi_{E,i,j} = \sum_{i=1}^N \left(p_A \alpha (A_{t,i,j}^*)^\beta (L_{t,i,j}^*)^\phi + p_E (F - A_{t,i,j}^*) - w L_{t,i,j}^* - C_A A_{t,i,j}^* \right) \quad (17)$$

Total annual REDD + expenditures on PES are also calculated for a given household enrollment rate in the program. Because welfare is calculated at the household level, Equation (17) can easily be used to compare the impacts of REDD + payments in terms of equity across household socioeconomic groups (e.g., richest versus poorest).

LUCC allocation submodel: Once the optimal agricultural land area is defined, farmer-agents decide what LUCC needs to take place to adjust land use on their farms to that value. When deforestation is required, farmer-agents first clear secondary forest patches, with preference to patches with higher deforestation suitability (closer to previously established agricultural areas). If all secondary forest patches are cleared and the optimal amount of land in agricultural use is still not yet reached, farmer-agents convert mature forest patches, also giving preference to patches with higher deforestation suitability, until the optimal land-use level is reached or until the entire farm is under agricultural use. When the optimal amount of agriculture land is less than the amount previously used for agriculture in the farm, farmer-agents abandon agricultural patches, affording priority to patches with higher abandonment suitability (closer to forested areas), until the optimal level is reached. Finally, the size of each land-use/cover class and the net carbon balance from the LUCC processes (CO₂ emissions minus sequestration) are reported at the equilibrium state of the model.

2.4. Model verification and sensitivity analysis

Model verification was conducted for debugging purposes (Wilensky and Rand, 2015). Local sensitivity analysis was conducted to examine which parameters most affect simulation results (Railsback and Grimm, 2012). Sensitivity analysis of this model was particularly important because parameter values were either empirically estimated with the 2009 panel data and assumed to be constant through the simulations, or obtained from studies based on different regions of the Amazon Basin (Tables 1 and 2). Sensitivity was analyzed based on the relative change of the following model parameters and their effects on the optimal level of agricultural land at the equilibria: Cobb-Douglas production function parameters; price of the agricultural output; agricultural costs; net carbon emission factor; REDD + payments; discount rate; and, hypothetical carbon project lifetime (see Equations (1)–(3)). For each step of the sensitivity analyses, all independent variables were held constant except the variable of interest, which assumed original values decreased and increased by 100% from base value by 10% intervals. The analysis was conducted under both the carbon market-based and the REDD + policy payment-based option schemes. Additionally, a sensitivity analysis of the artificial neural network-based model used to create the deforestation suitability map for the mature forest was conducted with TerrSet v.18.11 software. The latter analysis was based on three methods: (1) forcing a single independent variable to be constant at each step of the analysis; (2) forcing all independent variables except one to be constant at each step of the analysis; and, (3) *Backwards Stepwise Constant Forcing*. The latter procedure initiates the analysis by holding constant every variable to determine which has the least effect on model accuracy. It then tests every possible pair of variables that include the one with the least effect to identify which pair of variables has the least effect on accuracy when held constant. The procedure is repeated holding an extra variable constant at each step until only one variable remains (Eastman, 2015).

2.5. Model validation

Face and empirical validations were conducted at micro- and macroscales. In accordance with Wilensky and Rand (2015), face validation involves demonstration that the model's mechanics and properties correspond to the mechanics and properties observed in the studied system, as assessed through visual interpretation, while the empirical validation is based on simulated and real numerical

data comparisons. Similarly, microvalidation evaluates whether the behaviors and mechanisms encoded into the farmer-agents match real farmer analogs, while macrovalidation checks whether the emergent simulated behaviors from the model correspond to aggregated behaviors observed at the landscape level.

At the microscale, face validation focused on the magnitude of the optimal area of deforestation observed during simulations, while the empirical validation compared the simulated annual household revenues, costs, and profits with their analogs obtained from the 2009 panel data (Caviglia-Harris et al., 2014). Only a proportion of the products harvested were sold, and that proportion is not captured in Equation (1). Therefore, the proportion of products sold (θ) was empirically estimated and discounted from the outcome of the profit function to render model estimates comparable to the panel data (Table 2). At the macroscale, the model was face validated through pattern comparison of LUCC simulation maps at baseline equilibrium (without REDD + payments) and the most recent LUCC classification map (2010) available from time series prepared by Toomey et al. (2013). Empirical validation was conducted with the *Figure of Merit* method (Pontius et al., 2008). The latter is a straightforward way to assess a LUCC model's prediction accuracy. Its calculation is based on the proportion of the area of agreements between satellite-based and simulation maps over the sum of agreements and the area of disagreement between the same two maps. LUCC models assessed with the *Figure of Merit* method generally exhibit prediction accuracy <50% (e.g., Fuller et al., 2011; Kim, 2010; Li et al., 2012; Müller and Mburu, 2009; Vieilledent et al., 2013), but the proposed model faced an additional limitation to validation insofar as households had not necessarily reached their optimal LUCC configurations by 2010. Furthermore, recent changes in the Brazilian Forest Code (Soares-Filho et al., 2014), increasing efforts to control illegal deforestation (Brasil, 2013, 2008), and the creation of conservation incentives (Soares-Filho et al., 2016) might reduce the once widespread failures of compliance with forest conservation regulations in Amazonian Brazil (Fearnside, 2005). These changes could imply that the total farm area available for conversion to agriculture (F) should be altered to capture the minimum forested area that households must preserve (e.g., $0.8 \cdot F$). However, these factors have arguably not yet affected the historical patterns of poor conformance with environmental regulations by small farm households (Nunes et al., 2015). In any case, the fact that the proposed model does not account for ongoing LUCC in Brazil is another source of uncertainty in validation.

Table 1
Parameter estimates for the production function.

	Agricultural production (Mg ha ⁻¹)			
	all data	outliers excluded	all data	outliers excluded
Labor (persons year ⁻¹)	0.15*** (0.05)	0.17*** (0.05)	0.16*** (0.05)	0.18*** (0.04)
Agricultural area reported by the household (ha)	0.45*** (0.06)	0.51*** (0.05)		
Agricultural area estimated with remote sensing (ha)			0.40*** (0.06)	0.42*** (0.06)
Constant	0.97*** (0.21)	0.72*** (0.20)	1.07*** (0.24)	0.99*** (0.22)
Observations	531	524	536	529
R ²	0.12	0.18	0.09	0.11
Adjusted R ²	0.12	0.17	0.09	0.11
Residual Std. Error	1.02 (d.f. = 528)	0.93 (d.f. = 521)	1.05 (d.f. = 533)	0.98 (d.f. = 526)
F Statistic	37.66*** (d.f. = 2; 528)	51.63*** (d.f. = 2; 521)	26.87*** (d.f. = 2; 533)	33.99*** (d.f. = 2; 526)

Note: *p < 0.10; **p < 0.05; ***p < 0.01; standard errors are noted in parentheses; d.f. = degrees of freedom.

Table 2
Model parameters.

Parameter	Notation	Value	Source
Cobb-Douglas production function	α	2.63	Panel data (Caviglia-Harris et al., 2014, Table 1)
	β	0.45	Panel data (Caviglia-Harris et al., 2014, Table 1)
	φ	0.15	Panel data (Caviglia-Harris et al., 2014, Table 1)
Net carbon emission or sequestration from the conversion of forest to agricultural land or the converse, respectively	δ	433 Mg CO ₂ ha ⁻¹	Baccini et al. (2012; Figs. S3 and S4), Mokany et al. (2006), and Fearnside (1996)
Price of rice-equivalent	p_A	R\$1.3 kg ⁻¹	Panel data (Caviglia-Harris et al., 2014; Fig. S7)
Proportion of rice-equivalents sold in the market	θ	59%	Panel data (Caviglia-Harris et al., 2014)
Price of the environmental service payments	p_E	US\$10 Mg CO ₂ ⁻¹	Hamrick and Goldstein (2016, 2009 exchange rate: 2 R\$/US\$)
Wages	w	R\$25 day ⁻¹	Panel data (Caviglia-Harris et al., 2014)
Discount rate	r	10%	Table S6
Labor cost of deforestation and land preparation	γ	38 person day ha ⁻¹	Walker (2003)
Maintenance cost of previously established agricultural areas	C_A	R\$ 114 ha ⁻¹	Panel data (Caviglia-Harris et al., 2014)
Non-labor cost of deforestation	C_D	R\$ 50 ha ⁻¹	Estimated ^a (Barreto et al., 1998; Walker, 2003; West et al., 2014, 1998 exchange rate: 1.16 R\$/US\$)

^a Non-labor cost of deforestation was based on the cost to operate chainsaws reported by Barreto et al. (1998), US\$5.7 day⁻¹ for 116.6 m³ day⁻¹ for two persons. Considering the average volume felled per hectare reported for the same area (37.4 m³ ha⁻¹; West et al., 2014), each feller was estimated to cover on average 1.6 ha day⁻¹. Hence, the non-labor cost of deforestation was estimated at \$3.7 day⁻¹ ha⁻¹ chainsaw⁻¹. Given the average reported Walker (2003) of 11.8 person-day ha⁻¹ for the tree-felling activity associated with deforestation and assuming that each person carries a chainsaw, the final non-labor cost of deforestation was estimated at US\$43.1 ha⁻¹ in 1998.

3. Results

Simulated maps successfully mimicked LUCC patterns observed on deforestation frontiers. At the baseline equilibrium state, the entire deforestation frontier region was cleared. As REDD + payments become a factor at the household-level LUCC-decision making, patches of forest appear at the equilibrium state. When increases in costs of agricultural and deforestation activities result in financial losses, deforestation does not occur and agricultural areas are abandoned (Figs. 2 and 6). The LUCC patterns observed in the simulated landscape are similar to the “fishbone” patterns observed in the real study area and other deforestation frontier regions (Roberts et al., 2002).

3.1. Empirical parameter estimation

The parameters of the production function estimated with an ordinary-least squares regression resulted in the following equation (Table 1):

$$f(A_t, L_t) = 2.63 \cdot A_t^{0.45} L_t^{0.15} \quad (18)$$

in which all parameters were significantly and positively correlated with the production outcome. Other empirically estimated parameters were based on the average or weighted-average values from the panel data. Parameters that could not be estimated were based on values reported in the literature (Tables 1 and 2; Figs. S5 and S7).

3.2. Sensitivity analysis results

Distinct but expected simulation behaviors resulted from changes in parameter settings during the sensitivity analysis (Figs. 3 and 4). At equilibrium, parameters α , β , and φ from the Cobb-Douglas production function and the sale price of agricultural outputs (p_A) were all positively correlated with the optimal agricultural area (ha). This result is expected because increasing any of these variables increases the potential revenue obtained from agricultural land for a given amount of area and labor. Among these parameters, β , which determines how the agricultural area affects rice-equivalent production, was the most sensitive – to the point that its effect on the optimal agricultural area was the only one that required expression on a logarithmic scale. As expected, increases

in production and crop prices led to higher profits, which sustains agricultural land use, covers deforestation expenses, and reduces the efficacy of REDD + payments. In contrast, financial and labor costs associated with maintenance of agricultural patches (w and C_A), deforestation (w , C_D , and γ), and the discount rate (r) were all negatively correlated with the optimal area in agriculture. Intuitively, when labor/non-labor costs increase, maintaining agricultural land becomes prohibitively expensive and deforestation is no longer a profitable LUCC decision. Similarly, the amount of REDD + payments (p_E) and, for the carbon market scheme payment option, the net carbon emission factor associated with the conversion from forest to agricultural land use or the net carbon sequestration factor from the conversion from agriculture to forest (δ ; Table 2) were also negatively correlated with the optimal agricultural area. As REDD + payments or carbon stocks increase compared to the stocks on agricultural lands (baseline), the forest conservation option becomes more attractive to households. Lastly, the REDD + project lifetime (T), under the carbon market scheme option, was positively correlated with the optimal agricultural area. This effect reflects the assumption that a given ton of CO₂ for which REDD + payments have been made will only become eligible for additional payments under a new carbon project lifetime.

Based on the relationships established by the artificial neural networks model, in all three sensitivity analyses of the model used to create the deforestation suitability map, distance from previous deforested areas was the most influential biophysical variable to inform the location of future LUCC, while the administrative areas at the municipality level was the least influential. The order of importance of the other biophysical variables varied by the sensitivity analysis method employed (Tables S7–S10).

3.3. Model validation results

The optimal area of deforestation simulated by the model conformed to expectations. At the baseline equilibrium, entire farms are converted to agricultural land. Most important, for the model's empirical microvalidation, the estimated agricultural household annual revenues (average = \$4927), costs (average = \$2155), and profits (average = \$2772) from the profit function differed little from the revenues (average = \$5390), costs (average = \$2429), and profits (average = \$2961) obtained from the panel data ($p = 0.44$, 0.25, and 0.73, respectively; Fig. 5).

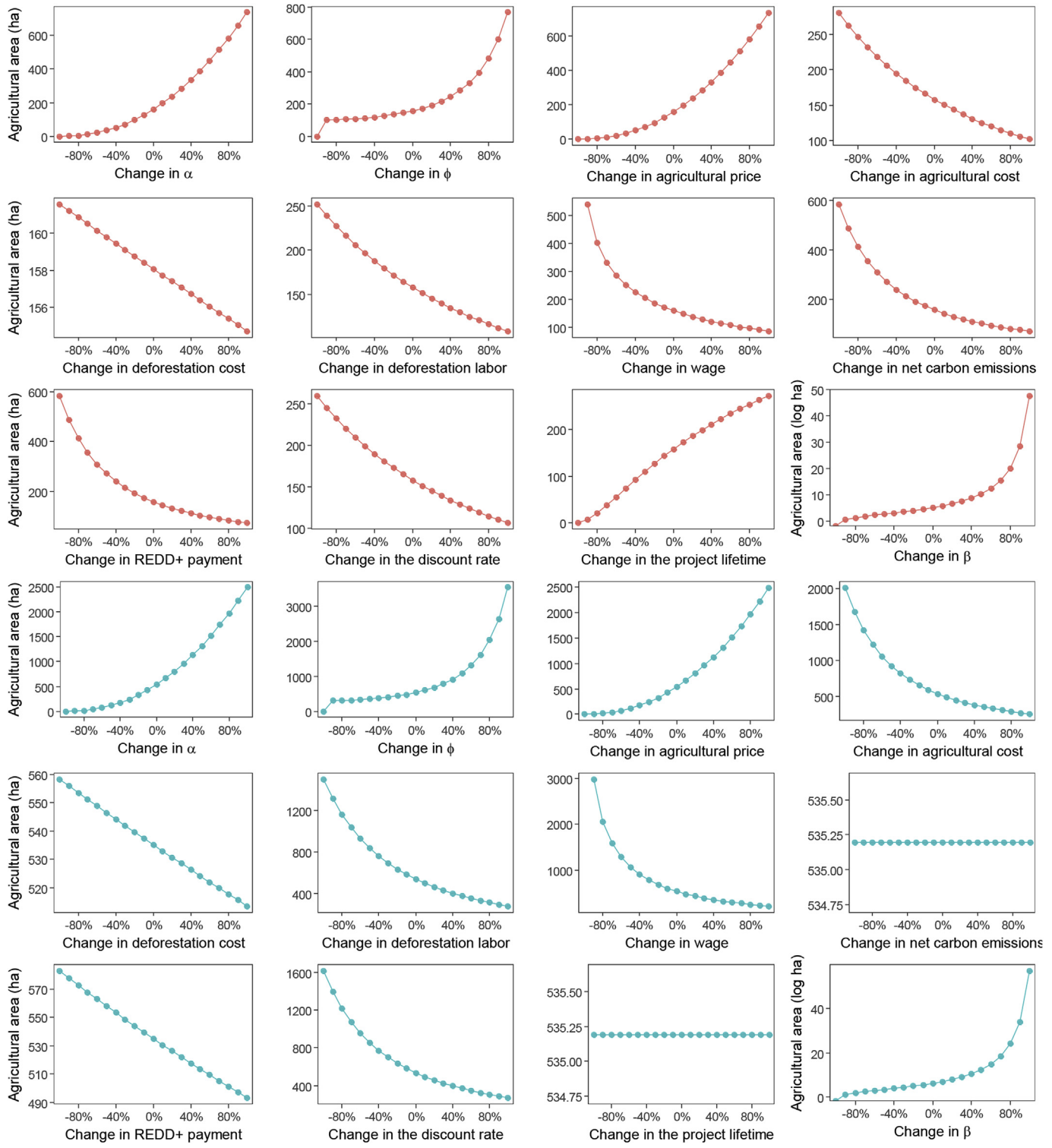


Fig. 3. Sensitivity analysis under the carbon market payment option (red lines) and the REDD+ policy payment option (blue lines). (For interpretation of the references to colour in this figure legend, the reader is referred to the web version of this article.)

The “fishbone” patterns of deforestation that emerged during the simulations provide good evidence to support the model’s face macrovalidation. Furthermore, despite the limitations of adopting the *Figure of Merit* for the spatially explicit and empirical macro-validation of the model at equilibrium, the prediction accuracy score was reasonably high (59%; Fig. 6).

4. Discussion

The most critical component of a LUCC-ABM is arguably the decision-making processes of its agents. Many decision-making processes in such models are based on decision trees (Acosta et al., 2014; Deadman et al., 2004; Salvini et al., 2016). In contrast,

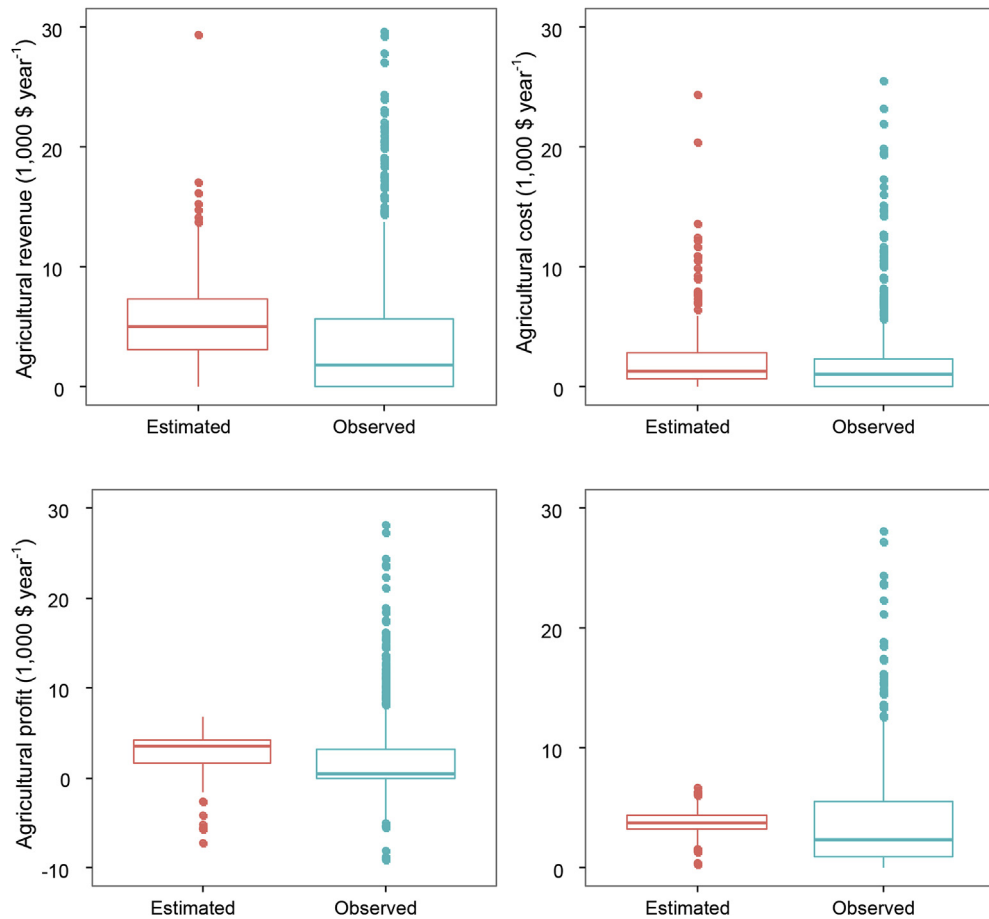


Fig. 4. Empirical microvalidation of the model. Red boxplots represent the outcomes estimated by the profit function, while blue boxplots represent the values reported by the household. Outliers excluded for enhanced visualization. In the last right panel, observations with negative agricultural profits were excluded. (For interpretation of the references to colour in this figure legend, the reader is referred to the web version of this article.)

the model presented here adopted a microeconomic framework based on the assumption that perfectly market-integrated households behave as profit maximizers. Consequently, the decision-making process was framed as a dynamic optimization problem, like those often adopted in the environmental and natural resource economics literature (e.g., Amit, 1986; Barbier, 1999; Brown, 2008). A potential criticism of the profit maximization assumption is that many theories of farm households posit them as utility maximizers rather than profit maximizers (Barnum and Squire, 1979; Chayanov, 1926; Taylor and Adelman, 2003). Using these theories, a household's utility is often captured as a function of trade-offs between consumption and leisure constrained by limited access to labor markets. These characteristics are not necessarily accurate representations of farm households on the old deforestation frontier of the Ouro Preto do Oeste region where labor markets function well. As demonstrated in the microeconomic household models of deforestation developed by Angelsen (1999), the utility maximization behavior can be reduced to profit maximization under perfect labor market conditions. Profit or utility maximization dichotomy aside, we acknowledge that the optimizing behavior assumption itself does not fully explain human decision-making (Jager et al., 2000; Le et al., 2008). Alternatives to maximization behaviors discussed in the literature include (i) achieving minimum levels of satisfaction or (ii) decision trees, where agents repeat the same action until they run out of resources such as labor or capital (Deadman et al., 2004; Salvini et al., 2016). Furthermore, an additional stochastic factor could be added to the final optimal LUCC

calculation as an attempt to mimic imperfect household decisions or a stochastic optimization approach based on the generation and use of random variables could be adopted (e.g., Ermolieva et al., 2015).

The key component of the profit function incorporated into the model LUCC decision-making process is the agricultural production function. While the functional form of the production function can affect the behavior of the farmer-agents (Angelsen, 1999), a Cobb-Douglas form was chosen due to its closed solution properties and widespread use in the farm household and LUCC literature (Angelsen, 1999; Darwin et al., 1996). Despite the numerous data transformations required for the conversion of heterogeneous household production outputs to the rice-equivalent, the production function generated parameter values similar to those in the literature. For example, in the function estimated by Barnum and Squire (1979) for paddy rice farmers in Malaysia, the respective β and φ associated with the agricultural land size and labor were estimated as 0.62 and 0.29. Although, the overall fit of our function was somewhat low ($R^2 = 0.12$) compared to others in the literature based on single-crop systems (e.g., $R^2 = 0.67$ reported by the previous authors), the simulated annual agricultural revenue did not differ substantially from the values in the panel data reported by the households in the region (Caviglia-Harris et al., 2014). Additionally, the global concavity of the profit function ensured that the simulation had achieved a maximum. Finally, the sensitivity analysis of the model parameters did not reveal unexpected or contradictory outcomes.

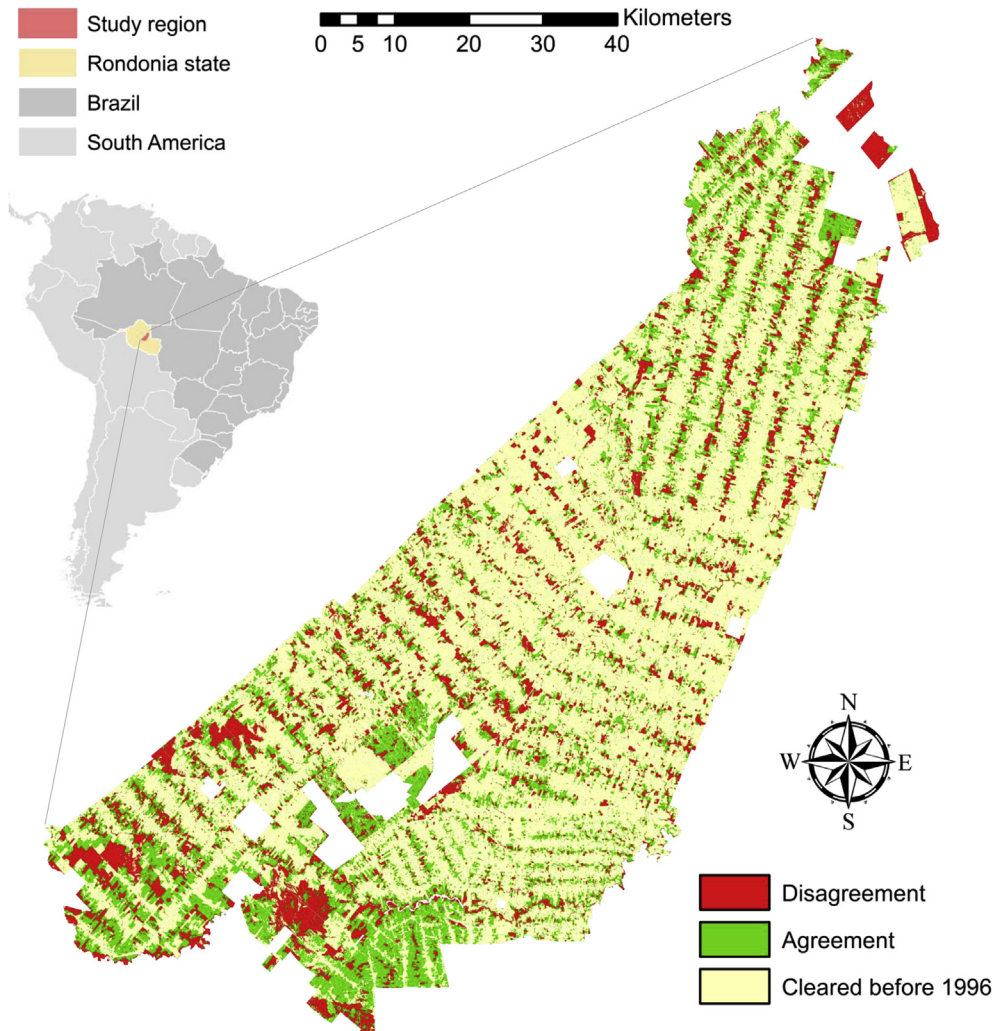


Fig. 5. Agreements and disagreements between simulated post-1996 deforestation at equilibrium state and the satellite-based post-1996 deforestation in 2010. Agreements represent areas predicted and as deforested where deforestation occurred. Disagreements represent areas predicted as deforested where deforestation did not occur.

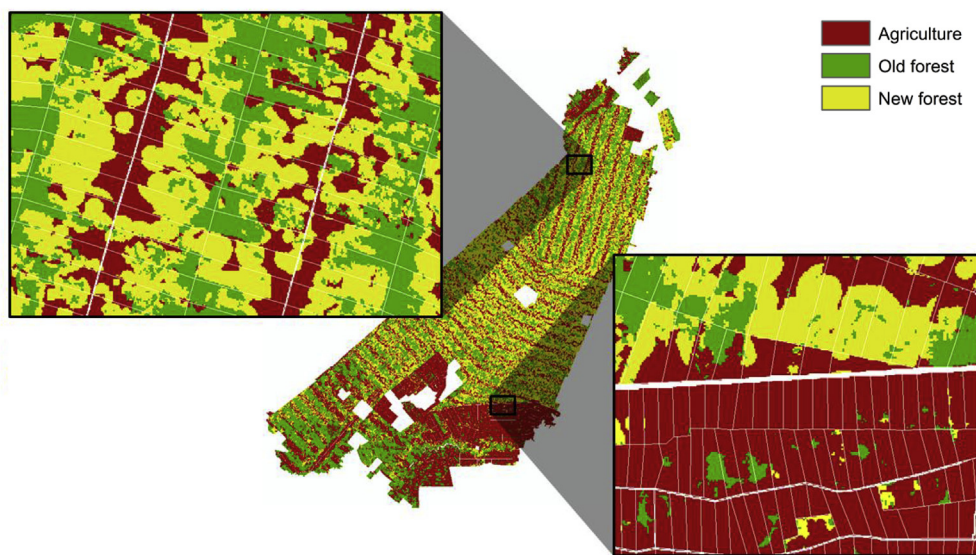


Fig. 6. Land-use/cover patterns within farms from the REDD + payment simulations. Left window displays how agricultural areas tend to be close to roads. Right window contrasts the effects of REDD + payments on large versus small lots. Old forests represent the mature forest patches present at the beginning of the simulation. New forests represent the areas of forest regrowth in 1996 plus the agricultural areas allocated to forest regrowth throughout the simulation assume to reach the status of mature forest at model equilibrium.

The fact that our production function does not discriminate between family and hired labor combined with the assumption of perfect labor markets implies that households are treated as homogenous agents. Such characteristics are arguably in contrast to general LUCC-ABMs that are often based on heterogeneity and stochasticity (An, 2012; Le et al., 2008). Nevertheless, heterogeneity is incorporated into the model through the LUCC allocation submodel, as expansion of agricultural land is constrained by farm size (F), which varies across settlements. For instance, the first orthogonal (i.e., fishbone arrangement) settlements from the 1970s were 100 ha lots, while the newer ones follow a radial pattern with each land holding approximately 12 ha (Caviglia-Harris and Harris, 2011).

The LUCC allocation submodel generated the “fishbone” deforestation patterns in the simulations since REDD + payments caused shifts in land-use/cover equilibria at the landscape level. Based on sensitivity analyses of the artificial neural networks-model used to create the deforestation suitability map, distance from previously deforested areas was the most influential biophysical variable explaining the location of observed deforestation (between 1986 and 1996), followed by distance from protected areas and elevation. These results are in agreement with a recent meta-analysis about the drivers of deforestation conducted by Ferretti-Gallon and Busch (2014) and other similar studies (Müller et al., 2012; Pfaff, 1999; Soares-Filho et al., 2010). The *Figure of Merit* of this model was high compared to others in the literature and in comparison to those for decentralized/private REDD projects. For instance, Pontius et al. (2008) found that close to one-third of the LUCC models they tested produced *Figures of Merit* <10% with only one >50%. Similarly, an assessment of deforestation models conducted by Kim (2010) found no *Figure of Merit* >8% for a highly deforested area in Santa Cruz, Bolivia. The median *Figure of Merit* from 41 model validation runs conducted by Fuller et al. (2011) for the peat swamp forests of Central Kalimantan, Indonesia, was 17%, while Li et al. (2012) reported a 27% *Figure of Merit* for simulated scenarios of biofuel-crops expansion in the Great Plains states of the United States. Müller and Mburu (2009) found *Figures of Merit* ranging 37–41% after substantially large training cycles to forecast LUCC in the Kakamega Forest of Western Kenya, while the deforestation simulations for Madagascar carried out by Vieilledent et al. (2013) achieved values of 10–23%. However, the spatially explicit validation of *SimREDD* + benefited from the regional context of the study in one of the most degraded old deforestation frontiers in the Brazilian Amazon (Toomey et al., 2013). So much forest clearing has occurred in the study region that the 2010 LUCC classification map could be empirically validated against the LUCC model output at the baseline equilibrium state.

The implications of starting the model with the 1996 LUCC configurations are somewhat important. There were three main reasons for the selection of 1996 as the first year of the model. First, it precedes the year when the Kyoto Protocol – the first international climate mitigation agreement – was signed at the 7th Conference of Parties to the United Nations Framework Convention on Climate Change (UNFCCC, 1998) and discussions of whether or not to include mitigation activities based on avoided deforestation were still underway (Tolba and Rummel-Bulsko, 1998). Second, it matches the first year of the panel data collection in the settlements of the Ouro Preto do Oeste region (Caviglia-Harris et al., 2014). Third, it allows the model to begin with a large area of mature forest in the virtual landscape, which gives the model flexibility to predict deforestation and/or reforestation (Fig. S1). Abandonment of agricultural patches occurs in the equilibrium state if a household has previously established more agricultural land than the optimal level dictated in the scenario settings. The abandonment decision can result from two distinct implications of the model settings.

Households abandon farmed land when (1) revenues are lower than costs and agricultural production is not lucrative or (2) when REDD + payments exceed agricultural profits. Both settings imply that farmer-agents set aside part of their agricultural land so that their new mixture of agricultural land and forest area maximizes profit.

Simulations from the model present a REDD + payment framework similar to the current (2017) situation. The REDD + policy payment scheme is based on annual payments for forest area maintained or recovered, which is similar to PES program in countries like Costa Rica, Ecuador, and Mexico (Arriagada et al., 2012; de Koning et al., 2011; Honey-Rosés et al., 2009; Torres et al., 2013). In contrast, the carbon market option assumes payments based on net carbon emissions avoided (Mg CO₂). This option, in accordance with carbon accounting methodologies proposed by the Intergovernmental Panel on Climate Change (IPCC, 2006, 2003), the United Nations Framework Convention on Climate Change (UNFCCC, 2013a, 2013b, 2007), and the standards and methodologies for decentralized/private REDD + initiatives developed for the voluntary carbon market (e.g., Avoided Deforestation Partners, 2012; Pedroni, 2012; Verified Carbon Standard, 2017b). Numerous ongoing examples of REDD + projects that follow the latter payment option are also described in the literature (e.g., West, 2016). Settings for three key model parameters determine whether households are better off with the former or the latter REDD + payment option: (1) the net carbon emissions factor (δ); (2) the length of the hypothetical REDD + project (T); and, (3) the size of REDD + payments (p_E). For instance, the *Monarch Butterfly Conservation Fund* in Mexico offered annual conservation payments of \$12 ha⁻¹ of forest (Honey-Rosés et al., 2009), while the average carbon offset price in the voluntary carbon market was \$3.30 Mg CO₂⁻¹ in recent reports, with a range between minimum and maximum prices of \$21.60 CO₂⁻¹ (Hamrick and Goldstein, 2016). The length of the decentralized/private REDD + projects is often in agreement with the 20–100 year range set by the leading voluntary carbon standard, the Verified Carbon Standard (Goldstein and Neyland, 2015; Verified Carbon Standard, 2017b). Lastly, aboveground biomass stocks, which are used as references for estimating avoided net carbon emission, vary substantially across tropical forests, with averages from 40 to 310 Mg ha⁻¹ (Baccini et al., 2012; IPCC, 2006). The distinct values and ranges presented above illustrate the variety of potential scenarios that can lead to substantially different LUCC and welfare outcomes given the PES scheme adopted. Hence, the proposed model, with its two payment options, can provide meaningful insights into the design and potential outcomes of REDD + initiatives.

5. Conclusion

A hybrid optimization-ABM model was proposed to investigate the effects of REDD + payments on LUCC and community welfare in settlements on an old deforestation frontier in Brazil. The model, built into an ABM platform, is based on two distinct submodels, one for the dynamic LUCC optimization decision and the other for identification of areas suitable for land-use/cover change and persistence within the households' lots in the study region. The optimization submodel, which assumes households behave as profit maximizers under perfect labor markets, was calibrated empirically with unbalanced socioeconomic panel data. The key component of the profit function maximized by the farmer-agents in the model is the Cobb-Douglas production function, based on a standard crop output (the rice-equivalent), and function of agricultural area and labor. While the dynamic optimization process returns deterministic and homogenous results for the farmer-

agents, differences in household landholdings and initial land-use/cover configurations incorporate heterogeneity into the model. The outcome of the model is the optimal land-use/cover configuration for households at the equilibrium state taking into account the revenues from REDD + payments based on the conservation of forest areas and promotion of natural regeneration. This submodel allows for the quantification of changes in forest cover and agricultural production in response to different REDD + payment options, as well as a means to calculate the changes in welfare at the community level, which is tightly related to equity issues associated with PES. The LUCC allocation submodel was constructed with an artificial neural networks-based algorithm and spatially explicit biophysical variables correlated with LUCC observed between 1986 and 1996. The latter submodel is responsible for the emergence of the classic “fishbone” patterns of deforestation observed in the output of the simulations when REDD + payments occur. Results from this submodel can estimate impacts of REDD + payments on habitat fragmentation and biological conservation at the landscape level. The submodel can also serve for the identification and ranking of forest areas more threatened by future deforestation. A key feature of *SimREDD+* is its ability to simulate two distinct and widely adopted REDD + payment options, one based on forest and forest regrowth areas ($\$ \text{ ha}^{-1}$), in accordance with national REDD + -like conservation programs, and the other based on avoided net carbon emissions and net carbon sequestration ($\$ \text{ Mg CO}_2^{-1}$), in conformance with voluntary carbon market rules.

As expected, without REDD + payments, and with the assumption of continued widespread non-compliance with environmental regulations, the land-use/cover at equilibrium state is complete conversion of forests to agricultural land. When REDD + payments are incorporated into the simulation, forest patches appear in the virtual landscape at model equilibria. Similar results are observed as agricultural and deforestation costs increase or as agricultural revenues decrease. These results indicate the mechanics behind the model are in conformance to what we would expect to observe in reality. Overall, the model can serve as a virtual impact evaluation tool to explore the effects of PES interventions intended to impede deforestation. Impacts can be measured in terms of LUCC, greenhouse gas emissions, program enrollment and costs, food production, and community welfare. Hence, *SimREDD +* can shed light on a wide range of topics, e.g., natural resource economics and governance, rural development, food security, landscape ecology, habitat fragmentation, climate change mitigation, and equity studies. Insights from simulation scenarios can improve the design of more effective, efficient, and equitable REDD + programs and initiatives that involve farm household participation.

Acknowledgements

This research was funded by the National Science Foundation (grant SES-0752936). Additional funds to the first author were provided by the Brazilian National Counsel of Technological and Scientific Development (CNPq; grant 201138/2012-3), the William C. and Bertha M. Cornett Fellowship and the Tropical Conservation and Development Graduate Assistantship at the University of Florida, and the World Wildlife Fund's Prince Bernhard Scholarship for Nature Conservation.

Appendix A. Analytical solution for the optimal agricultural land definition

The step-by-step analytical solution involves solving for λ_t in Equation (8):

$$\lambda_t = w\gamma + C_D + \psi \Leftrightarrow \dot{\lambda}_t = 0 \quad (19)$$

Since $\dot{\lambda}_t$ and λ_t are known, L_t is given recursively by Equation (9) as function of A_t :

$$p_A \beta \alpha A_t^{\beta-1} L_t^\varphi - p_E \delta - C_A - \psi = r(w\gamma + C_D + \psi) \quad (20)$$

$$L_t = \left(\frac{A_t^{1-\beta} (rC_D + p_E \delta + C_A + r\psi + rw\gamma + \psi)}{p_A \beta \alpha} \right)^{\frac{1}{\varphi}} \quad (21)$$

Once L_t is defined, the expression for the optimal agricultural land at equilibrium (A^*) is given recursively by Equation (7):

$$p_A \theta \varphi \alpha A_t^\beta \left(\left(\frac{A_t^{1-\beta} (rC_D + p_E \delta + C_A + r\psi + rw\gamma + \psi)}{p_A \beta \alpha} \right)^{\frac{1}{\varphi}} \right)^{\varphi-1} = w \quad (22)$$

$$A_t^* = \left(\frac{w \beta^{1-\frac{1}{\phi}} \alpha^{-\frac{1}{\phi}} p_A^{-\frac{1}{\phi}} (rC_D + p_E \delta + C_A + r\psi + rw\gamma + \psi)^{\frac{1}{\phi}-1}}{\phi} \right)^{\frac{\phi}{\beta+\phi-1}} \quad (23)$$

Appendix B. Supplementary data

Supplementary data related to this article can be found at <https://doi.org/10.1016/j.envsoft.2017.11.007>.

References

- Abram, N.K., MacMillan, D.C., Xofis, P., Ancrenaz, M., Tzanopoulos, J., Ong, R., Goossens, B., Koh, L.P., Del Valle, C., Peter, L., Morel, A.C., Lackman, I., Chung, R., Kler, H., Ambu, L., Baya, W., Knight, A.T., 2016. Identifying where REDD+ financially out-competes oil palm in floodplain landscapes using a fine-scale approach. *PLoS One* 11, 1–23.
- Acosta, L., Rounsevell, M.D.A., Bakker, M., Van Doorn, A., Gómez-Delgado, M., Delgado, M., 2014. An agent-based assessment of land use and ecosystem changes in traditional agricultural landscape of Portugal. *Intell. Inf. Manag.* 6, 55–80.
- Amit, R., 1986. Petroleum reservoir exploitation: switching from primary to secondary recovery. *Oper. Res.* 34, 534–549.
- An, L., 2012. Modeling human decisions in coupled human and natural systems: review of agent-based models. *Ecol. Modell.* 229, 25–36.
- An, L., Linderman, M., Qi, J., Shortridge, A., Liu, J., 2005. Exploring complexity in a human–environment system: an agent-based spatial model for multidisciplinary and multiscale integration. *Ann. Assoc. Am. Geogr.* 95, 54–79.
- Andersen, L., Bilge, U., Groom, B., Gutierrez, D., Killick, E., Ledezma, J.C., Palmer, C., Weinhold, D., 2014. Modelling Land Use, Deforestation, and Policy Analysis: a Hybrid Optimization-ABM Heterogeneous Agent Model with Application to the Bolivian Amazon. Centre for Climate Change Economics and Policy Working Paper (No. 186) (London).
- Angelsen, A., 1999. Agricultural expansion and deforestation-modelling the impact of population, market forces and property rights. *J. Dev. Econ.* 58, 185–218.
- Arriagada, R.A., Ferraro, P.J., Sills, E.O., Pattanayak, S.K., Cordero-Sancho, S., 2012. Do payments for environmental services affect forest cover? A Farm-level evaluation from Costa Rica. *Land Econ.* 88, 382–399.
- Avoided Deforestation Partners, 2012. REDD Methodological Module: Estimation of Baseline Carbon Stock Changes and Greenhouse Gas Emissions from Unplanned Deforestation (BL-UP) (v1.0) (Washington, D.C.).
- Baccini, A., Goetz, S.J., Walker, W.S., Laporte, N.T., Sun, M., Sulla-Menashe, D., Hackler, J., Beck, P.S.A., Dubayah, R., Friedl, M.A., Samanta, S., Houghton, R.A., 2012. Estimated carbon dioxide emissions from tropical deforestation improved by carbon-density maps. *Nat. Clim. Chang.* 2, 182–185.
- Barbier, E.B., 1999. Endogenous growth and natural resource scarcity. *Environ. Resour. Econ.* 14, 51–74.
- Barnum, H.N., Squire, L., 1979. An econometric application of the theory of the farm-household. *J. Dev. Econ.* 6, 79–102.
- Barreto, P., Amaral, P., Vidal, E., Uhl, C., 1998. Costs and benefits of forest management for timber production in eastern Amazonia. *For. Ecol. Manag.* 9–26.

Blackman, A., 2013. Evaluating forest conservation policies in developing countries using remote sensing data: an introduction and practical guide. *For. Policy Econ.* 34, 1–16.

Börner, J., Baylis, K., Corbera, E., Ezzine-de-Blas, D., Ferraro, P.J., Honey-Rosés, J., Lapeyre, R., Person, U.M., Wunder, S., 2016. Emerging evidence on the effectiveness of tropical forest conservation. *PLoS One* 11, 1–11.

Börner, J., Wunder, S., 2008. Paying for avoided deforestation in the Brazilian Amazon: from cost assessment to scheme design. *Int. For. Rev.* 10, 496–511.

Börner, J., Wunder, S., Wertz-Kanounnikoff, S., Hyman, G., Nascimento, N., 2014. Forest law enforcement in the Brazilian Amazon: costs and income effects. *Glob. Environ. Chang.* 29, 294–305.

Borrego, A., Skutsch, M., 2014. Estimating the opportunity costs of activities that cause degradation in tropical dry forest: implications for REDD+. *Ecol. Econ.* 101, 1–9.

Brasil, 2013. Atualização do Plano Nacional sobre Mudança do Clima. Comitê Interministerial sobre Mudança do Clima, Brasília.

Brasil, 2008. Plano Nacional sobre Mudança do Clima. Comitê Interministerial sobre Mudança do Clima, Brasília.

Bronfenbrenner, M., Douglas, P.H., 1939. Cross-section studies in the Cobb-Douglas function. *J. Polit. Econ.* 47, 761–785.

Brown, D.R., 2008. A spatiotemporal model of shifting cultivation and forest cover dynamics. *Environ. Dev. Econ.* 13, 643–671.

Caviglia-Harris, J., Harris, D., 2011. The impact of settlement design on tropical deforestation rates and resulting land cover patterns. *Agric. Resour. Econ. Rev.* 40, 451–470.

Caviglia-Harris, J., Roberts, D., Sills, E., 2014. Longitudinal Survey Data of Households in Ouro Preto Do Oeste, Rondonia, Brazil, 1996–2009 (Ann Arbor).

Caviglia-Harris, J.L., 2005. Cattle accumulation and land use intensification by households in the Brazilian Amazon. *Agric. Resour. Econ. Rev.* 34, 145–162.

Caviglia-Harris, J.L., 2004. Household production and forest clearing: the role of farming in the development of the Amazon. *Environ. Dev. Econ.* 9, 181–202.

Caviglia-Harris, J.L., Toomey, M., Harris, D.W., Mullan, K., Bell, A.R., Sills, E.O., Roberts, D.A., 2015. Detecting and interpreting secondary forest on an old Amazonian frontier. *J. Land Use Sci.* 10, 442–465.

Chayanov, A.V., 1926. *The theory of Peasant Economy*. The University of Wisconsin Press, Madison.

Dale, V.H., O'Neill, R.V.R.V., Southworth, F., Pedlowski, M., Pedlowski, F.M., 1994. Modeling effects of land management in the Brazilian Amazonian settlement of Rondônia. *Conserv. Biol.* 8, 196–206. <https://doi.org/10.1046/j.1523-1739.1994.08010196.x>.

Darwin, R., Tsigas, M., Lewandrowski, J., Raneses, A., 1996. Land use and cover in ecological economics. *Ecol. Econ.* 17, 157–181.

Deadman, P., Robinson, D., Moran, E., Brondizio, E., 2004. Colonist household decisionmaking and land-use change in the Amazon Rainforest: an agent-based simulation. *Environ. Plan. B Plan. Des.* 31, 693–709.

de Koning, F., Aguinaga, M., Bravo, M., Chiu, M., Lascano, M., Lozada, T., Suarez, L., 2011. Bridging the gap between forest conservation and poverty alleviation: the Ecuadorian Socio Bosque program. *Environ. Sci. Policy* 14, 531–542.

Eastman, R., 2015. *TerrSet Manual* (Worcester).

Ermolieva, T.Y., Ermoliev, Y.M., Havlik, P., Mosnier, A., Leclerc, D., Kraksner, F., Khabarov, N., Obersteiner, M., 2015. Systems analysis of robust strategic decisions to plan secure food, energy, and water provision based on the stochastic globiom model. *Cybern. Syst. Anal.* 51, 125–133.

ESRI, 2015. ArcGIS Desktop (v10.3.1). Environmental Systems Research Institute.

Evans, T.P., Manire, A., De Castro, F., Brondizio, E., McCracken, S., 2001. A dynamic model of household decision-making and parcel level landcover change in the eastern Amazon. *Ecol. Modell.* 143, 95–113.

Farmer, J.D., Foley, D., 2009. The economy needs agent-based modelling. *Nature* 460, 685–686.

Fearnside, P.M., 2005. Deforestation in brazilian Amazonia: history, rates, and consequences. *Conserv. Biol.* 19, 680–688.

Fearnside, P.M., 1996. Amazonian deforestation and global warming: carbon stocks in vegetation replacing Brazil's Amazon forest. *For. Ecol. Manage.* 80, 21–34.

Ferretti-Gallon, K., Busch, J., 2014. What Drives Deforestation and What Stops it? a Meta-analysis of Spatially Explicit Econometric Studies. Center for Global Development Working Paper (No. 361) (Washington, D.C.).

Fuller, D.O., Hardjono, M., Meijaard, E., 2011. Deforestation projections for carbon-rich peat swamp forests of Central Kalimantan, Indonesia. *Environ. Manage.* 48, 436–447.

Geist, H.J., Lambin, E.F., 2002. Proximate causes and underlying driving forces of tropical deforestation. *Bioscience* 52, 143.

Goldstein, A., Neyland, E., 2015. Converging at the Crossroads: State of Forest Carbon Finance 2015 (Washington, D.C.).

Grimm, V., Berger, U., DeAngelis, D.L., Polhill, J.G., Giske, J., Railsback, S.F., 2010. The ODD protocol: a review and first update. *Ecol. Model.* 221, 2760–2768.

Hamrick, K., Goldstein, A., 2016. Raising Ambition: State of the Voluntary Carbon Markets 2016 (Washington, D.C.).

Honey-Rosés, J., López-García, J., Rendón-Salinas, E., Peralta-Higuera, A., Galindo-Leal, C., 2009. To pay or not to pay? Monitoring performance and enforcing conditionality when paying for forest conservation in Mexico. *Environ. Conserv.* 36, 120.

Ickowitz, A., Sills, E., de Sassi, C., 2017. Estimating smallholder opportunity costs of REDD+: a pantropical analysis from households to carbon and back. *World Dev.* 95, 15–26.

IPCC, 2006. Forest land. In: 2006 IPCC Guidelines for National Greenhouse Gas Inventories. IPCC, Hayama, pp. 4.1–4.83.

IPCC, 2003. Good Practice Guidance for Land Use, Land-Use Change and Forestry, Intergovernmental Panel on Climate Change, Good Practice Guidelines on Land Use, Land Use Change and Forestry. Institute for Global Environmental Strategies (IGES) for the IPCC, Hayama.

Iwamura, T., Lambin, E.F., Silvius, K.M., Luzar, J.B., Fragoso, J.M.V., 2016. Socio-environmental sustainability of indigenous lands: simulating coupled human–natural systems in the Amazon. *Front. Ecol. Environ.* 14, 77–83.

Iwamura, T., Lambin, E.F., Silvius, K.M., Luzar, J.B., Fragoso, J.M.V., 2014. Agent-based modeling of hunting and subsistence agriculture on indigenous lands: understanding interactions between social and ecological systems. *Environ. Model. Softw.* 58, 109–127.

Jager, W., Janssen, M.A., De Vries, H.J.M., De Greef, J., Vlek, C.A.J., 2000. Behaviour in commons dilemmas: Homo economicus and Homo psychologicus in an ecological-economic model. *Ecol. Econ.* 35, 357–379.

Kim, O.S., 2010. An assessment of deforestation models for reducing emissions from deforestation and forest degradation (REDD). *Trans. GIS* 14, 631–654.

Kindermann, G., Obersteiner, M., Sohngen, B., Sathaye, J., Andrasko, K., Rametsteiner, E., Schlamadinger, B., Wunder, S., Beach, R., 2008. Global cost estimates of reducing carbon emissions through avoided deforestation. *Proc. Natl. Acad. Sci.* 105, 10302–10307.

Le, Q.B., Park, S.J., Vlek, P.L.G., Cremer, A.B., 2008. Land-Use Dynamic Simulator (LUDAS): a multi-agent system model for simulating spatio-temporal dynamics of coupled human-landscape system. I. Structure and theoretical specification. *Ecol. Inf.* 3, 135–153.

Li, R., Guan, Q., Merchant, J., 2012. A geospatial modeling framework for assessing biofuels-related land-use and land-cover change. *Agric. Ecosyst. Environ.* 161, 17–26.

Li, J., Dietz, T., Carpenter, S.R., Folke, C., Alberti, M., Redman, C.L., Schneider, S.H., Ostrom, E., Pell, A.N., Lubchenco, J., Taylor, W.W., Ouyang, Z., Deadman, P., Kratz, T., Provencher, W., 2007. Coupled human and natural systems. *Ambio* 36, 639–649.

Luttrell, C., Sills, E., Aryani, R., Ekaputri, A.D., Evinke, M.F., 2017. Beyond opportunity costs: who bears the implementation costs of reducing emissions from deforestation and degradation? *Mitig. Adapt. Strateg. Glob. Chang.* 1–20.

Mena, C.F., Walsh, S.J., Frizzelle, B.G., Xiaozheng, Y., Malanson, G.P., 2011. Land use change on household farms in the Ecuadorian Amazon: design and implementation of an agent-based model. *Appl. Geogr.* 31, 210–222.

Michel, P., 1982. On the transversality condition in infinite horizon optimal problems. *Econometrica* 50, 975–985.

Mokany, K., Raison, R.J., Prokushkin, A.S., 2006. Critical analysis of root: shoot ratios in terrestrial biomes. *Glob. Chang. Biol.* 12, 84–96.

Monticino, M., Acevedo, M., Callicott, B., Cogdill, T., Lindquist, C., 2007. Coupled human and natural systems: a multi-agent-based approach. *Environ. Model. Softw.* 22, 656–663.

Müller, D., Mburu, J., 2009. Forecasting hotspots of forest clearing in Kakamega forest, western Kenya. *For. Ecol. Manage.* 257, 968–977.

Müller, R., Müller, D., Schierhorn, F., Gerold, G., Pacheco, P., 2012. Proximate causes of deforestation in the Bolivian lowlands: an analysis of spatial dynamics. *Reg. Environ. Chang.* 12, 445–459.

Nepstad, D.C., Soares-Filho, B.S., Merry, F., Moutinho, P., Rodrigues, H.O., Bowman, M.S., Schwartzman, S., Almeida, O.T., Rivero, S., 2007. The Costs and Benefits of Reducing Carbon Emissions from Deforestation and Forest Degradation in the Brazilian Amazon (Falmouth).

Ngo, A., See, L.M., 2012. Calibration and Validation of Agent-based Models of Land Cover Change, Agent-based Models of Geographical Systems.

Nunes, S.S., Barlow, J., Gardner, T.A., Siqueira, J.V., Sales, M.R., Souza, C.M., 2015. A 22 year assessment of deforestation and restoration in riparian forests in the eastern Brazilian Amazon. *Environ. Conserv.* 42, 193–203.

Pana, A.C., Gheysens, J., 2016. Baseline choice and performance implications for REDD+. *J. Environ. Econ. Policy* 5, 79–124.

Parker, D.C., Manson, S.M., Janssen, M.A., Hoffmann, M.J., Deadman, P., 2003. Multi-agent systems for the simulation of land-use and land-cover change: a review. *Ann. Assoc. Am. Geogr.* 93, 314–337.

Pedroni, L., 2012. Methodology for Avoided Unplanned Deforestation (v.1.1) (Washington, D.C.).

Pfaff, A.S.P., 1999. What drives deforestation in the brazilian Amazon? *J. Environ. Econ. Manage.* 37, 26–43.

Phan, T.H.D., Brouwer, R., Davidson, M., 2014. The economic costs of avoided deforestation in the developing world: a meta-analysis. *J. For. Econ.* 20, 1–16.

Pontius, R.G., Boersma, W., Castella, J.C., Clarke, K., Nijss, T., Dietzel, C., Duan, Z., Fotsing, E., Goldstein, N., Kok, K., Koomen, E., Lippitt, C.D., McConnell, W., Mohd Sood, A., Pijanowski, B., Pithadia, S., Sweeney, S., Trung, T.N., Veldkamp, A.T., Verburg, P.H., 2008. Comparing the input, output, and validation maps for several models of land change. *Ann. Reg. Sci.* 42, 11–37.

Pontius, R.G., Peethambaran, S., Castella, J.-C., 2011. Comparison of three maps at multiple resolutions: a case study of land change simulation in Cho Don District, Vietnam. *Ann. Assoc. Am. Geogr.* 101, 45–62.

Purnomo, H., Suyamto, D., Irawati, R.H., 2013. Harnessing the climate commons: an agent-based modelling approach to making reducing emission from deforestation and degradation (REDD)+work. *Mitig. Adapt. Strateg. Glob. Chang.* 18, 471–489.

R Core Team, 2016. R: a Language and Environment for Statistical Computing (v.3.3.0).

Railsback, S.F., Grimm, V., 2012. Agent-based and Individual-based Modeling a

Practical Introduction. Princeton University Press, Princeton.

Railsback, S.F., Lytinen, S.L., Jackson, S.K., 2006. Agent-based simulation platforms: review and development recommendations. *Simulation* 82, 609–623.

Rifai, S.W., West, T.A.P., Putz, F.E., 2015. “Carbon Cowboys” could inflate REDD+ payments through positive measurement bias. *Carbon Manag.* 6, 151–158.

Roberts, D.A., Numata, I., Holmes, K., Batista, G., Krug, T., Monteiro, A., Powell, B., Chadwick, O.A., 2002. Large area mapping of land-cover change in Rondonia using multitemporal spectral mixture analysis and decision tree classifiers. *J. Geophys. Res. D. Atmos.* 107, LBA 40-1–LBA 40-18.

Salvini, G., Ligtenberg, A., van Paassen, A., Bregt, A.K., Avitabile, V., Herold, M., 2016. REDD+ and climate smart agriculture in landscapes: a case study in Vietnam using companion modelling. *J. Environ. Manage.* 172, 58–70.

Sills, E.O., 2008. Evolution of the amazonian frontier: land values in Rondônia. *Braz. Land use policy* 26, 55–67.

Sills, E.O., de Sassi, C., Jagger, P., Lawlor, K., Miteva, D.A., Pattanayak, S.K., Sunderlin, W.D., 2017. Building the evidence base for REDD+: study design and methods for evaluating the impacts of conservation interventions on local well-being. *Glob. Environ. Chang.* 43, 148–160.

Snistveit, B., Stevenson, J., Villar, P., Eyers, J., Harvey, C., Panfil, S., Puri, J., McKinnon, M.C., 2016. Land-use Change and Forestry Programmes: Evidence on the Effects on Greenhouse Gas Emissions and Food Security (London).

Snooks, G.D., 2008. A general theory of complex living systems: exploring the demand side of dynamics. *Complexity* 13, 12–20.

Soares-Filho, B., Moutinho, P., Nepstad, D., Anderson, A., Rodrigues, H., Garcia, R., Dietzsch, L., Merry, F., Bowman, M., Hissa, L., Silvestrini, R., Maretti, C., 2010. Role of Brazilian Amazon protected areas in climate change mitigation. *Proc. Natl. Acad. Sci.* 107, 10821–10826.

Soares-Filho, B., Rajao, R., Macedo, M., Carneiro, A., Costa, W., Coe, M., Rodrigues, H., Alencar, A., 2014. Cracking Brazil's forest Code. *Sci.* 344, 363–364.

Soares-Filho, B., Rajao, R., Merry, F., Rodrigues, H., Davis, J., Lima, L., Macedo, M., Coe, M., Carneiro, A., Santiago, L., 2016. Brazil's market for trading forest certificates. *PLoS One* 11, 1–18.

Soares-Filho, B.S., Coutinho Cerqueira, G., Lopes Pennachin, C., 2002. DINAMICA - a stochastic cellular automata model designed to simulate the landscape dynamics in an Amazonian colonization frontier. *Ecol. Modell.* 154, 217–235.

Takasaki, Y., 2013. Deforestation, forest fallowing, and soil conservation in shifting cultivation. *Theor. Econ. Lett.* 3, 30–38.

Takasaki, Y., 2012. Economic models of shifting cultivation: a review. In: Moutinho, P. (Ed.), *Deforestation Around the World*. InTech, Rijeka, pp. 351–372.

Taylor, J.E., Adelman, I., 2003. Agricultural household models: genesis, evolution, and extensions. *Rev. Econ. Househ.* 1, 33–58.

Thompson, O.R.R., Paavola, J., Healey, J.R., Jones, J.P.G., Baker, T.R., Torres, J., 2013. Reducing emissions from deforestation and forest degradation (REDD+): transaction costs of six Peruvian projects. *Ecol. Soc.* 18, 17.

Tolba, M.K., Rummel-Bulsko, I., 1998. *Global Environmental Diplomacy: Negotiating Environment Agreements for the World, 1973–1992*. MIT Press, Cambridge.

Toomey, M., Roberts, D.A., Caviglia-Harris, J., Cochrane, M.A., Dewes, C.F., Harris, D., Numata, I., Sales, M.H., Sills, E., Souza, C.M., 2013. Long-term, high-spatial resolution carbon balance monitoring of the Amazonian frontier: predisturbance and postdisturbance carbon emissions and uptake. *J. Geophys. Res. Biogeosciences* 118, 400–411.

Torres, A.B., MacMillan, D.C., Skutsch, M., Lovett, J.C., 2013. Payments for ecosystem services and rural development: landowners' preferences and potential participation in western Mexico. *Ecosyst. Serv.* 6, 72–81.

UN-REDD, 2015. *Strategic Framework 2016–20* (Washington, D.C.).

UN-REDD, 2011. *The UN-REDD Programme Strategy 2011–2015* (Geneva).

UN-REDD, 2008. *Framework Document*. (Geneva).

UNFCCC, 2015. *Adoption of the Paris Agreement (Paris)*.

UNFCCC, 2013a. *Estimation of Carbon Stocks and Change in Carbon Stocks of Trees and Shrubs in A/R CDM Project Activities (v.04.1)* (Bonn).

UNFCCC, 2013b. *A/R Large-scale Consolidated Methodology Afforestation and Reforestation of Lands except Wetlands (V. 02.0)* (Bonn).

UNFCCC, 2007. *Tool for the Demonstration and Assessment of Additionality in A/R CDM Project Activities (v.02)*.

UNFCCC, 1998. *Kyoto Protocol* (Kyoto).

Verified Carbon Standard, 2017a. *Jurisdictional and Nested REDD+ (JNR) Requirements (v.3.4)* (Washington, D.C.).

Verified Carbon Standard, 2017b. *VCS Standard (v.3.7)* (Washington, D.C.).

Vieilledent, G., Grinand, C., Vaudry, R., 2013. Forecasting deforestation and carbon emissions in tropical developing countries facing demographic expansion: a case study in Madagascar. *Ecol. Evol.* 3, 1702–1716.

Walker, R., 2003. Mapping process to pattern in the landscape change of the amazonian frontier. *Ann. Assoc. Am. Geogr.* 93, 376–398.

West, T.A.P., 2016. Indigenous community benefits from a de-centralized approach to REDD+ in Brazil. *Clim. Policy* 16, 924–939.

West, T.A.P., Vidal, E., Putz, F.E., 2014. Forest biomass recovery after conventional and reduced-impact logging in Amazonian Brazil. *For. Ecol. Manage.* 314, 59–63.

Wilensky, U., 1999. *NetLogo (v.5.3.1)*.

Wilensky, U., Rand, W., 2015. *An Introduction to Agent-based Modeling: Modeling Natural, Social, and Engineered Complex Systems with NetLogo*. MIT Press (Cambridge, London).

Wolfram Research Institute, 2012. *Mathematica (v.9.0)*.